AN APPLICATION OF A NEW ELECTROMAGNETIC SENSOR TO REAL-TIME MONITORING OF FATIGUE CRACK GROWTH IN THIN METAL PLATES

M. Namkung, J. P. Fulton†, B. Wincheski† and C. G. Clendenin

NASA Langley Research Center
Hampton, VA 23681

† Analytic Services and Materials, Inc.
107 Research Dr., Hampton, VA 23666

INTRODUCTION

A major part of fracture mechanics is concerned with studying the initiation and propagation of fatigue cracks. This typically requires constant monitoring of crack growth during fatigue cycles which necessitates automation of the whole process. If the rate of crack growth can be determined the experimenter can vary externally controlled parameters such as load level, load cycle frequency and so on. Hence, knowledge of the precise location of the crack tip at any given time is very valuable. One technique currently available for measuring fatigue crack length is the DC potential drop method. The method, however, may be inaccurate if the direction of crack growth deviates considerably from what was assumed initially or the curvature of the crack becomes significant. Another approach is to digitize an optical image of the test specimen surface and then apply a pattern recognition technique to locate the crack tip, but this method is still under development.

The present work is an initial study on applying eddy current-type probes to monitoring fatigue crack growth. The performance of two types of electromagnetic probes, a conventional eddy current probe and a newly developed self-nulling probe, was evaluated for the detection characteristics at and near the tips of fatigue cracks. The scan results show that the latter probe provides a very well defined local maximum in its output in the crack tip region suggesting the definite possibility of precisely locating the tip, while the former provides a somewhat ambiguous distribution of the sensor output in the same region.

The paper is organized as follows: We start by reviewing the design and performance characteristics of the self-nulling probe and then describe the scan results which demonstrate the basic properties of the self-nulling probe. Next, we provide a brief description of the software developed for tracing a simulated crack and give a brief discussion of the main results of the test. The final section summarizes the major accomplishments of the present work and the elements of the future R&D needs.

DESIGN AND PERFORMANCE CHARACTERISTICS OF SELF-NULLING PROBE

As shown in Fig. 1, the self-nulling probe consists of an outer (driving) and an inner (pickup) coil separated by a cylindrical wall made of steel, called the flux-focusing lens. The probe used in the present study had a lens with an ID of 12.5 mm, a driving coil with 100 turns of AWG 28 copper wire, and a pickup coil with 600 turns of AWG 38 copper wire. The amplitude of the pickup coil output carries all the necessary flaw information and is the only

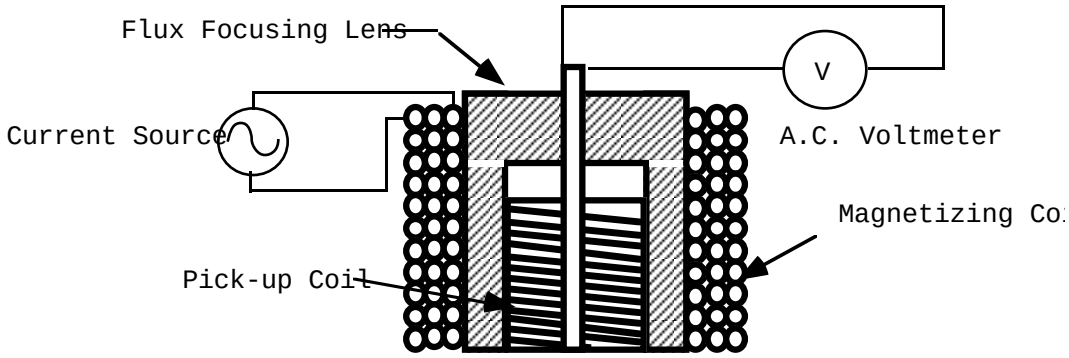

Fig. 1. Schematic diagram of the self-nulling probe.

parameter measured with this probe. Therefore, the actual instrumentation for the probe is very simple and straightforward. A function generator was used for the current source that activates the driving coil, and an oscilloscope was used to display the pickup coil output or an AC voltmeter was used whenever the measurement of the actual RMS voltage output was desired.

The presence of the ferrous wall is the key element that provides the unique performance characteristics shown in the next figure. Fig. 2. (a) shows the pickup coil output when the probe is held away from any conducting object (in air signal). The pickup coil output rapidly decreases as the probe is brought close to the crack free conducting surface, and then disappears when the probe is positioned on top of the sample as shown in Fig. 2. (b). The presence of a crack in the sample will disturb the balance between the applied field and the field due to eddy currents which reduces the nulling effect and produces a large pickup coil output as shown in Fig. 2.(c). Hence, the unambiguous detection of a crack can be accomplished with this probe using very simple instrumentation. Fig. 3. shows the deviation of the pickup coil output from the nulled state as a function of the distance between the probe and the surface of an aluminum plate. The results of Fig. 3 clearly indicate the insensitivity of the probe to lift-off.

The most unique feature of this new probe is the self-nulling capability that significantly simplifies the application procedure. This is due to the flux-focusing lens which shields the pickup coil and also generates concentrated eddy currents in a cylindrical region of the test specimen. A detailed analysis of the nulling effect can be found in two companion papers submitted to this conference. Hence, this paper will only concentrate on performance characteristics and applications of the probe.

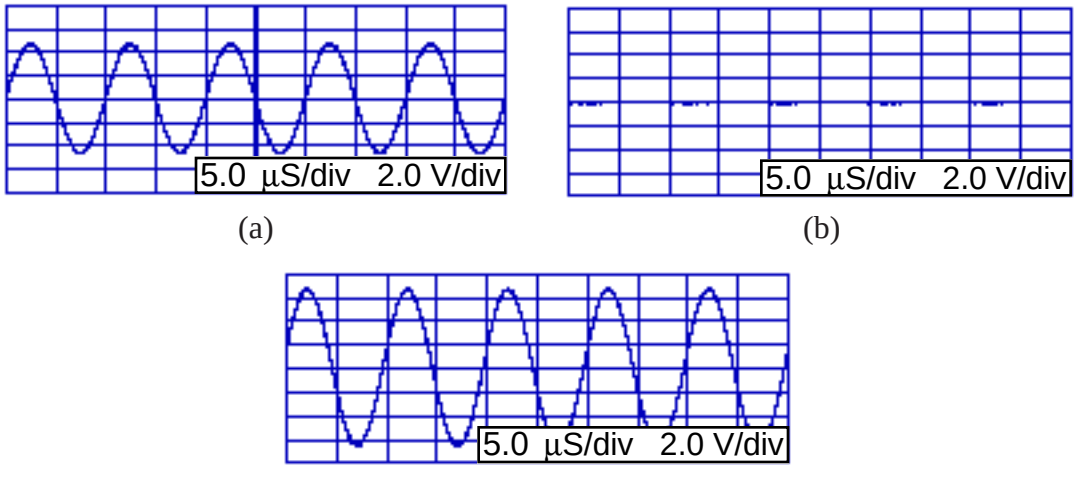

Fig. 2. (a). In-air pickup coil output (b). Nulled pickup coil output when the probe is positioned on a crack-free region of an aluminum plate (c). Pickup coil output at a crack due to a disturbance in the balance among the competing effects that caused the nulling of the output shown in (b).

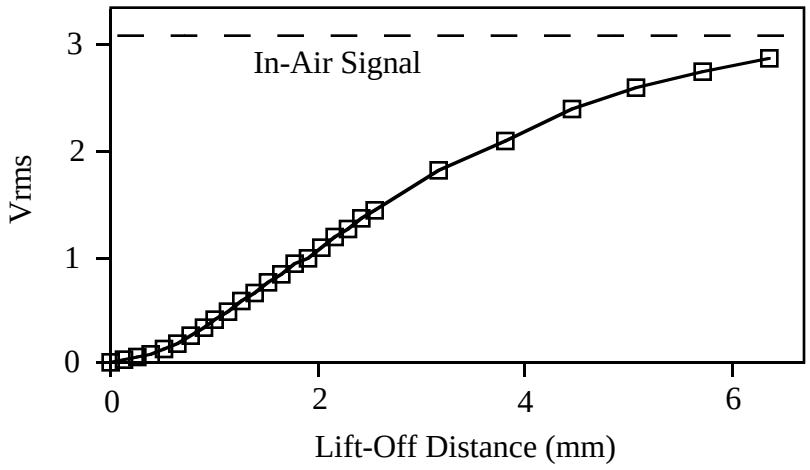

Fig. 3. Lift-off characteristics of the self-nulling probe.

Fig. 4 shows a schematic of the sample that was used to demonstrate the basic characteristics of the probe. Two 15 x 15 x 0.2 cm^3 aluminum plates were joined by four rivets. Two of the rivets, located diagonally opposite to one another, contained EDM notches. One rivet had a 1.5 mm long notch and the other had 0.5 mm long notch as measured from the rivet shank. The bottom plate of the sample had a 1.0 cm diameter hole in its center. Fig. 5 shows the image of the pickup coil output obtained by scanning a 1.25 cm diameter probe at an operating frequency of 72 kHz over the top surface of the sample. The image of the four rivets are clearly shown but only the 1.5 mm-long EDM notch was detected. Fig. 6 shows results obtained by using a 0.625 cm probe operating at 140 kHz. The image of each rivet becomes sharper and, due to the improved spatial resolution obtained by reducing the probe diameter, the presence of the 1.5 mm-long EDM notch is also visible. Fig. 7 shows the results of using a 1.25 cm diameter probe at an operating frequency of 10 kHz. At this frequency the induced eddy currents penetrate deeper into the material and the image of the

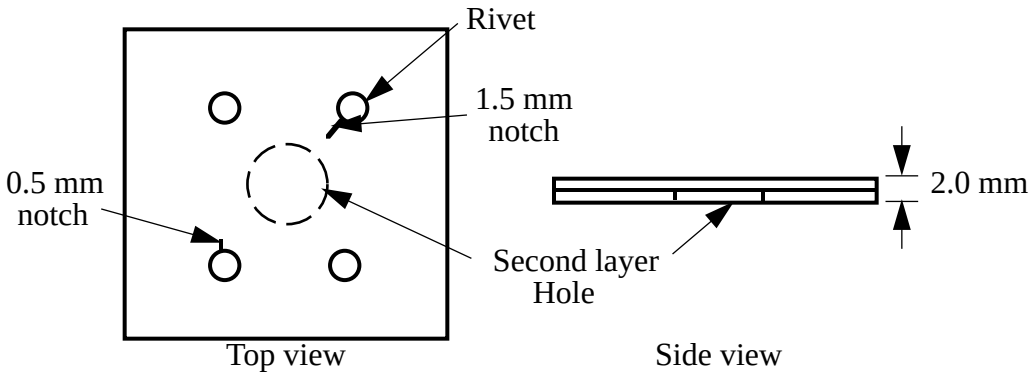

Fig. 4. Schematic illustration of the test sample used for scan images.

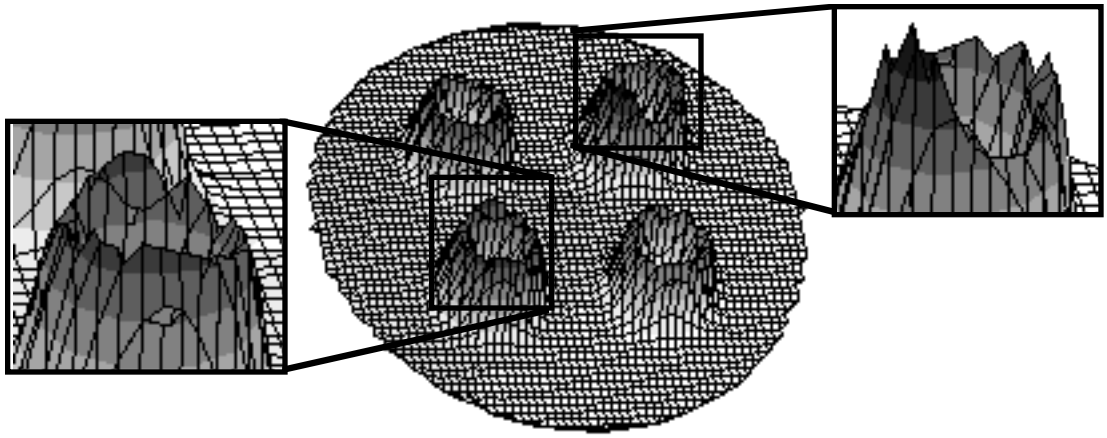

Fig. 5. Scan image of the sample in Fig. 4 obtained by using the 1.25 cm diameter probe operated at 72 kHz.

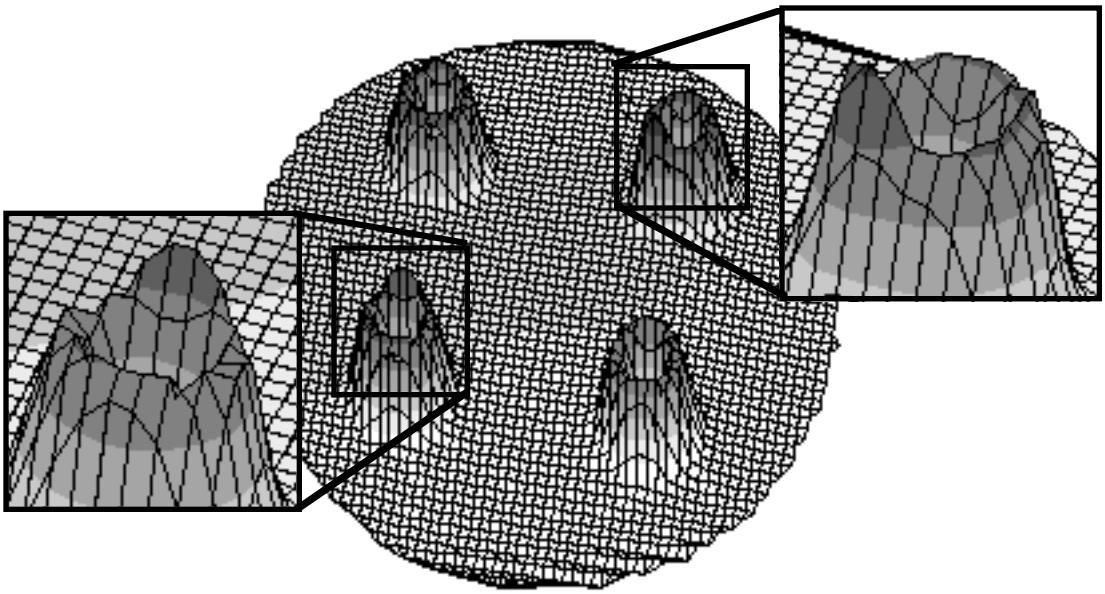

Fig. 6. Scan image obtained by using the.65 cm diameter probe operated at 140 kHz.

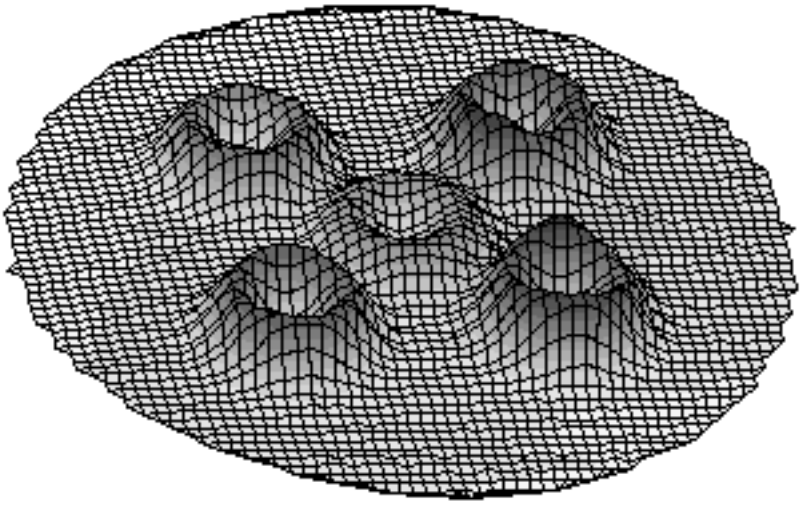

Fig. 7. Scan image obtained by using the 1.25 cm diameter probe operated at 10 kHz.

1.0 cm diameter center hole in the second plate can be seen. At the same time, the results clearly show that lowering the operating frequency reduces the nulling effect and also tends to broaden and blur the images due to flaws. We also note that the images of the rivets in Fig. 7 are much smoother than those shown in the two previous figures.The roughness in the images of the rivets taken at the higher operating frequencies may be due to varying degrees of mechanical contact between the rivet and the aluminum plate.

Additional test results were obtained by scanning over a sample which contained actual fatigue cracks. The sample was prepared from a 1.0 mm-thick aluminum plate with a rectangular size of 12.5 x 30 cm^2 and a centrally located 1.25 cm diameter hole. Small notches were made in two positions on the rim of this hole to initiate and grow cracks approximately perpendicular to the longer edge of the plate. Fig. 8. (a) shows the schematic of the resultant fatigue cracks while Fig. 8. (b) shows the scan test results obtained by using a 1.25 cm diameter probe operated at 50 kHz. We note that both images of the fatigue cracks clearly show a maximum in the vicinity of the crack tips. This is caused by eddy currents beneath the flux-focusing lens being diverted by the crack into the region directly under the pickup coil. Fig. 9. (a) illustrates more precisely what is happening. To better explain the phenomenon the resultant eddy current flow is decomposed into two separate complete rings of eddy currents flowing in an opposite sense in Fig. 9 (b). The role of the larger eddy current ring, which would have been the sole eddy current distribution in the absence of the crack, is to counter the effect of the applied magnetic field, while the smaller eddy current

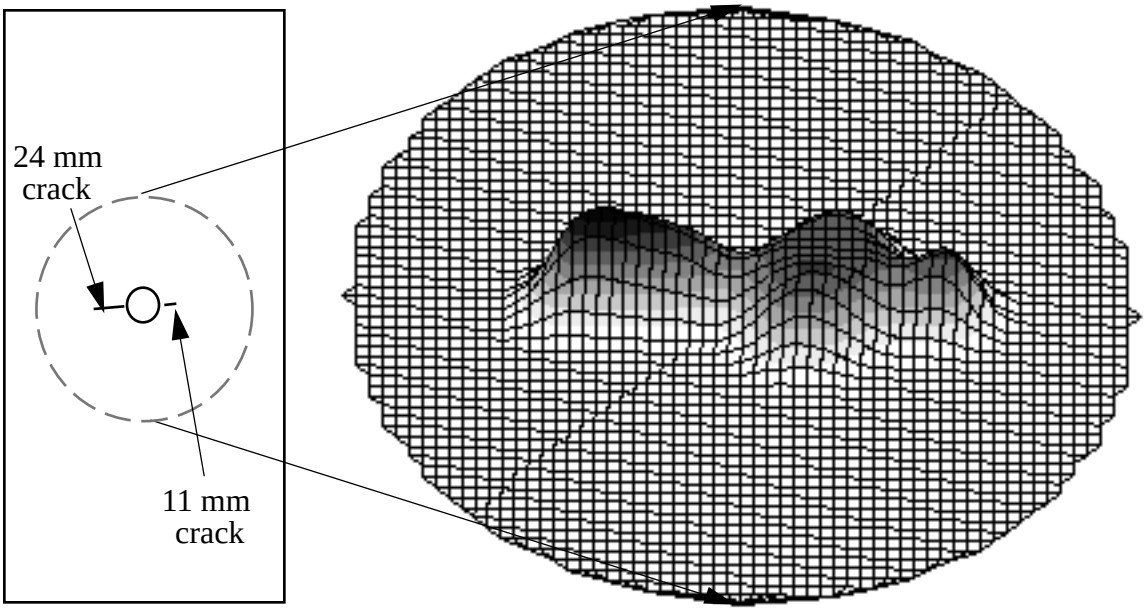

Fig. 8 (a). Schematic illustration of the geometry of the fatigue cracks. (b). Scan image of the fatigue cracks and center hole obtained using a 1.25 cm diameter probe at 50 kHz.

ring enhances the effect of the applied AC magnetic field. As a result, the probe output becomes largest near the crack tip.

To obtain more detailed information on the test results and confirm the presence of the local maximum output as a unique performance characteristic of the self-nulling probe the scan was repeated over a small area near the crack tip. For the purpose of comparison a conventional eddy current probe of 3.18 mm (1/8 inch) diameter was also used. For the latter measurement the probe output was rotated in the complex impedance plane such that the change due to lift-off is oriented in the horizontal axis (real component) and the variation in the vertical axis (imaginary component) was measured during the scan operation. Fig. 10. (a) shows the scan results obtained by using the 1.25 cm diameter self-nulling probe operated at 50 kHz where the line segment of AB is almost parallel to the crack while that of CD is approximately perpendicular to it. The distribution of the probe output along the segments AB and CD are shown in Fig. 10. (b) and (c), respectively. The distribution along the crack clearly shows a very well defined maximum at the crack tip. The scan test results of the conventional eddy current probe are shown in Fig. 11. (a), (b) and (c) in the same manner that the self-nulling probe test results were organized in the previous figure. The test results of the conventional eddy current probe do not show any local maximum in the probe output illustrating the above mentioned uniqueness of the self-nulling probe.

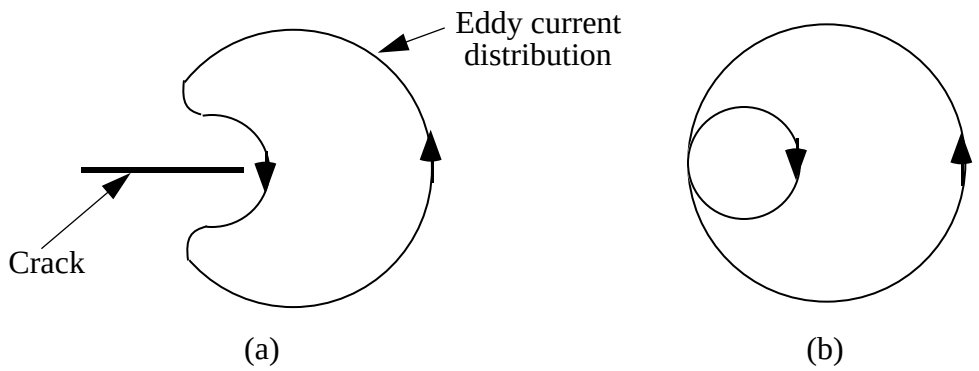

Fig. 9. (a). Eddy current flow which is altered near the crack tip. (b). Eddy current flow decomposed into two rings.

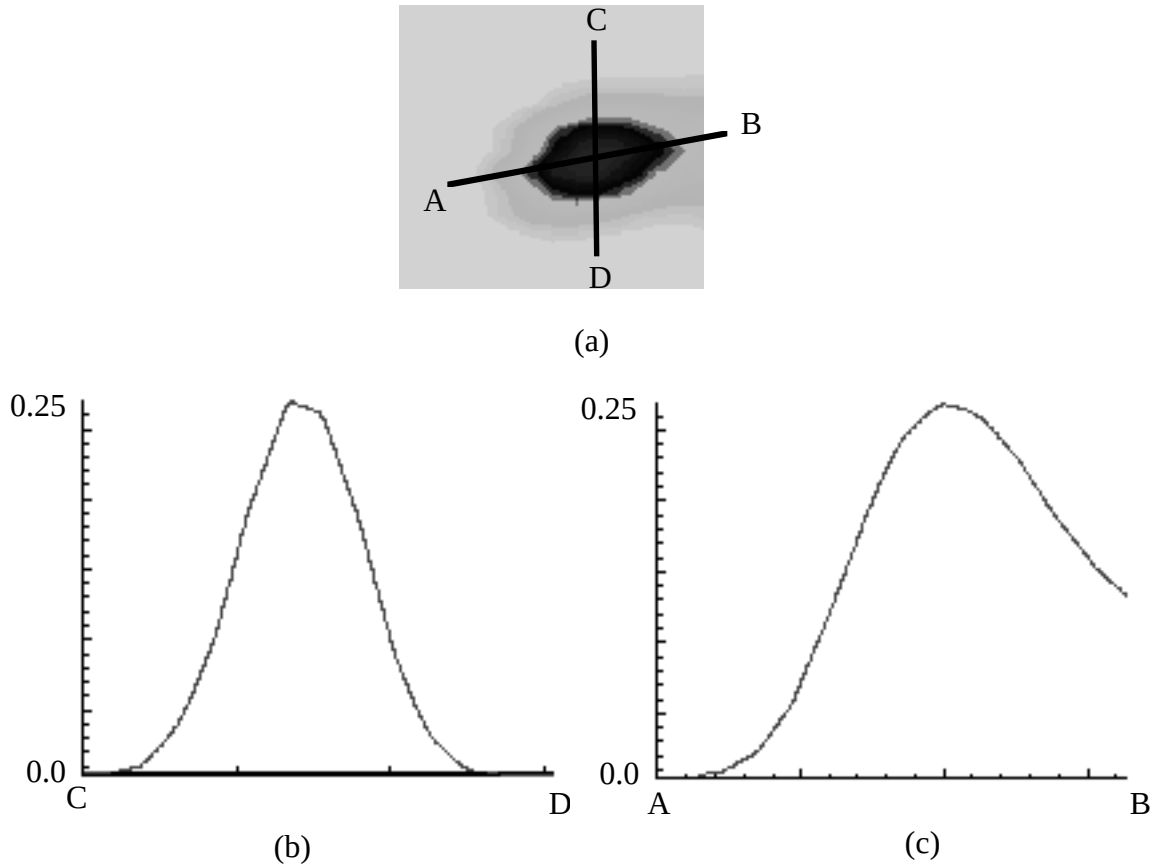

Fig. 10. (a). Two-dimensional representation of the scan test results of self-nulling probe where the segment AB is parallel and CD is perpendicular to the crack. (b) Probe output along the segment AB. (c). Probe output along the segment CD.

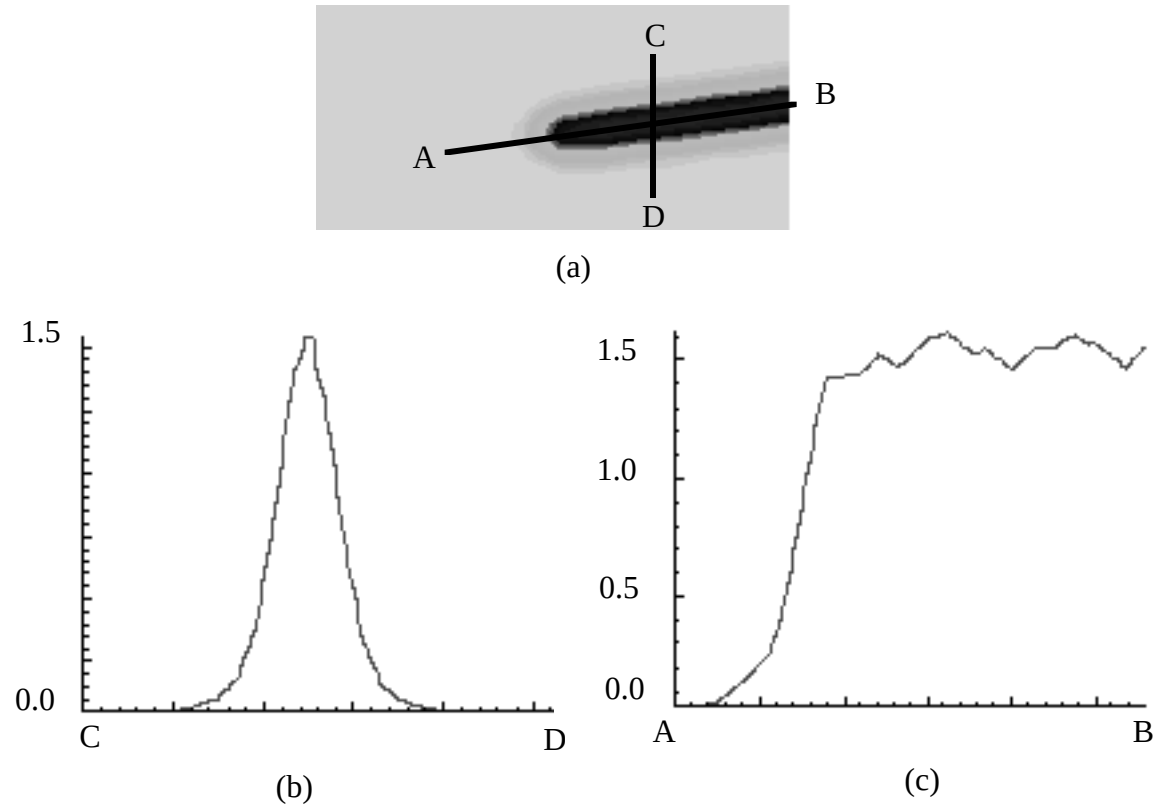

Fig. 11. (a). Two-dimensional representation of the scan test results of a conventional eddy current probe. (b). Probe output along segment AB. (c). Probe output along CD.

TRACING A SIMULATED CRACK

The original purpose of this study was to track the crack tip using the self-nulling electromagnetic probe as the crack grows during fatigue cycling. This, however, is a trivial task if one can locate the tip of a crack of any length. Hence, the emphasis of the present work was to demonstrate the capability of tracing a crack having a reasonable degree of complexity in its shape and in locating the crack tip. In this section the basic elements of the computer algorithm used for crack tracing will be described, the geometry of the simulated crack will be introduced, and the test results of locating the tip will be presented.

The crack tracing algorithm is based on the symmetry in the output as the probe moves across the crack as illustrated in Fig. 10. (b) and Fig. 11. (b). Initially the probe was placed roughly in the vicinity of the crack and we then let a scanner perform a vertical scan operation to search for a peak as the probe moved from $A \rightarrow B$ in Fig. 12, where the X-Y axes are set to correspond to the coordinate system of the scanner. Once the first peak, P_1, is found, the probe moves a small distance ΔL along the x-axis and repeats the vertical scan, which is indicated as $C \rightarrow D$ to find the second peak, P_2.One can assume that the line connecting these two point, P_1 and P_2, is very close to the tangential line of the crack at this local position. We choose the line connecting P_1 and P_2 as the new X'-axis and the orientation of the Y'-axis is automatically determined. The motion in the primed coordinate system was transformed back into the unprimed coordinate system for the scanner commands. The next step is to move the probe and perform the peak search as indicated by $E \rightarrow F$, which is along the Y'-axis. The process repeats, while choosing a new X' and Y' axis, based on the last two locations of the peak. In this way the possibility of the probe losing the crack and wandering away, from point P, for example, can be minimized. Finding the maximum output along the crack is a trivial task but the location of the maximum probe output does not exactly coincide with that of the crack tip. The geometrical relationship between these two points can be established either by computation or an empirical trial-and-error method. The latter method has been chosen for the present study and the details will be discussed later in this section.

To demonstrate the tracing capability of the technique an EDM notch of sufficient geometrical complexity has been made in an aluminum plate as shown in Fig. 13. The movement in the X'-axis was set to be 0.5 mm and every time the peak in the Y'-axis was detected its location was stored in the computer. The actual location of the crack tip slightly exceeds that of the probe output peak along the crack of Fig. 10 (c). It has been observed through repeated measurements that by stopping the probe motion where the probe output is 75% of the peak value we were able to locate the actual crack tip position within 0.8 mm (1/32 inch). In the actual tracing test about 5 cm of the initial range was skipped due to the limited range of the scanner as seen in the replotted test results shown in Fig. 14.

SUMMARY

The paper described one of the application areas of the newly developed self-nulling

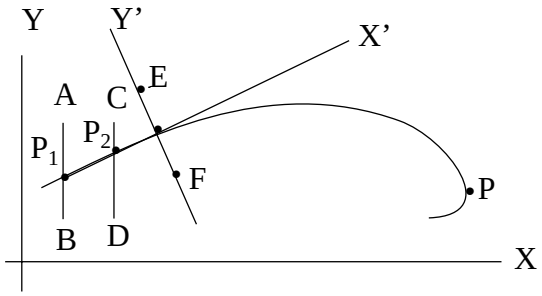

Fig. 12. Schematics of the fixed (unprimed) and moving (primed) coordinate systems for crack tracing.

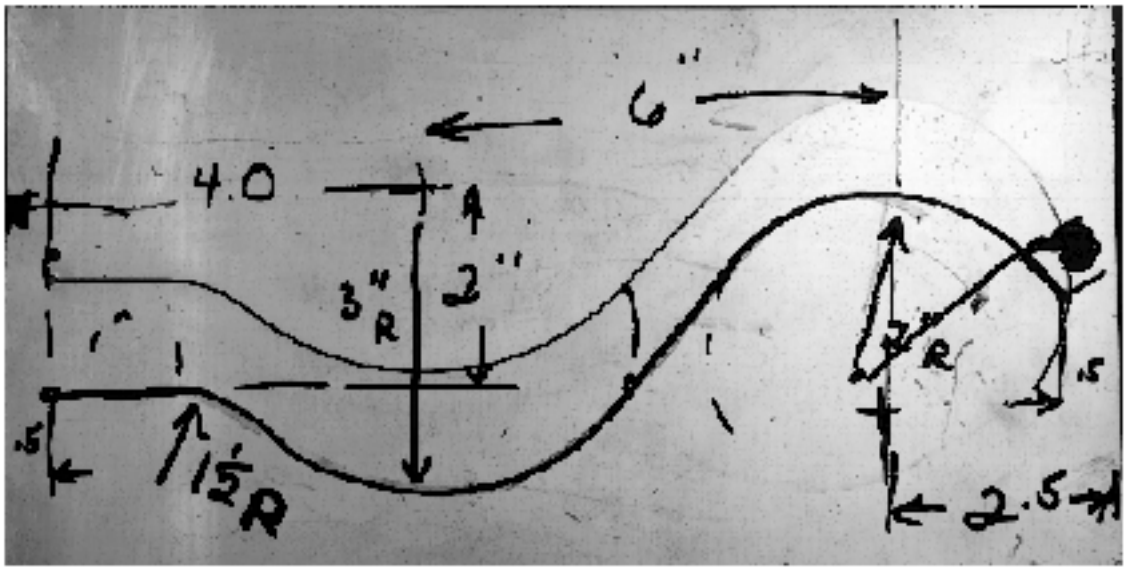

Fig. 13. Aluminum plate sample with a complex EDM notch.

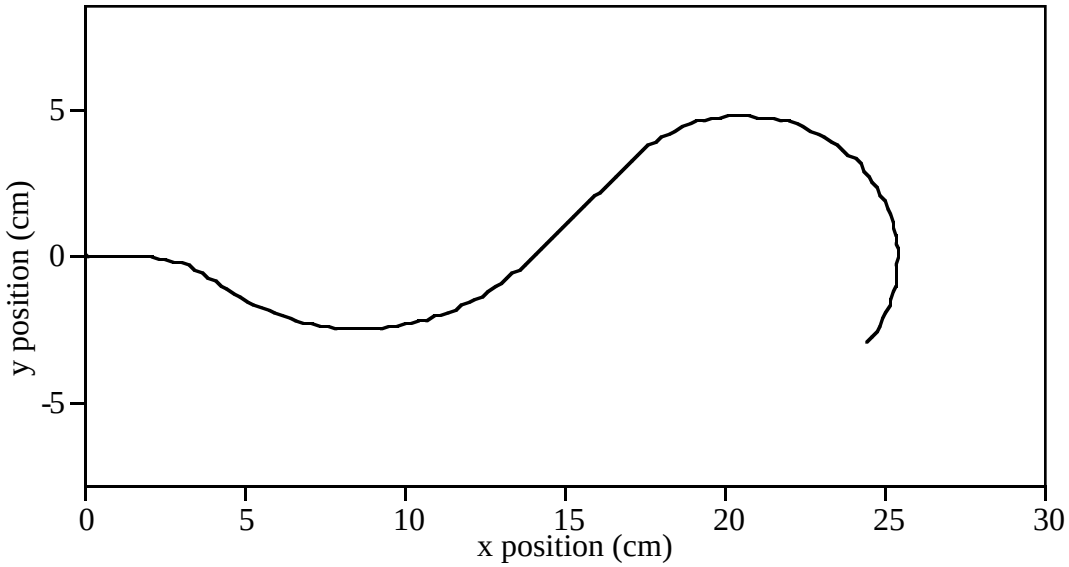

Fig. 14. Test results of crack tracing using the self-nulling probe.

electromagnetic probe that requires very simple instrumentation and test procedures. Tracing the tip of a fatigue crack in a thin aluminum plate, the self-nulling probe provides a very well defined probe output near the tip area whereas a conventional eddy current probe does not. The test results proved that it is possible to locate the crack tip within 0.8 mm based on empirical criteria. The computation of the actual probe output, based on 3-dimensional finite element modeling will be performed in the near future eliminating the need of relying on trial-and-error to determine the location of the maximum probe output.

REFERENCES

1. Private communication from R. Everette.
2. B. Wincheski, M. Namkung, J. P. Fulton and S. Nath, “New Eddy Current Probe for Thickness Gauging of Conductive Materials”, *Review of Progress in Quantitative NDE*, (this volume), edited by D. O. Thompson and D. E. Chimenti (Plenum Press, New York, 1993).
3. B. Wincheski, M. Namkung, J. P. Fulton, J. Simpson and S. Nath, “Characteristics of Ferromagnetic Flux Focusing Lens in The Development of Surface/Subsurface Flaw Detector”, *Review of Progress in Quantitative NDE*, (this volume), edited by D. O. Thompson and D. E. Chimenti (Plenum Press, New York, 1993).